Supporting information for the paper entitled:

$[Tc(CO)(CN\textit{p}\text{-}F\text{-}Ar^{DArF2})_4]^-$: an isocyanide analogue of the elusive $[Tc(CO)_5]^-$ anion

Federico Salsi,[a] Adelheid Hagenbach,[a] Joshua S. Figueroa,[b*] and Ulrich Abram[a*]

---

[a] Institute of Chemistry and Biochemistry, Freie Universität Berlin, Fabeckstr. 34/36, D-14195 Berlin Berlin, German

[b] Department of Chemistry and Biochemistry, University of California, San Diego, 9500 Gilman Drive Mail Code 0358, La Jolla CA, 92093-0358.

S1. Synthetic Procedures.

S1.1. General considerations. All manipulations were carried out under an argon atmosphere using standard Schlenk techniques. Unless otherwise stated, reagent-grade starting materials were purchased from commercial sources and either used as received or purified by standard procedures. Solvents were dried and degassed according to standard procedures. Glass fiber filters (Whatman) fixed with Teflon tape were employed for cannula filtration. CN*p*-F-Ar^{DArF2}, $(NBu_4)[Tc_2(CO)_6(\mu\text{-}Cl)_3]$ and [TcCl(CO)(CN*p*-F-Ar^{DArF2})$_4$] were prepared as previously described.[1-3]

NMR spectra were recorded at 20 °C with a JEOL 400 MHz multinuclear spectrometer. The values given for the ^{99}Tc and ^{19}F chemical shifts are referenced to pertechnetate and $CFCl_3$, respectively. THF-*d*$_8$ was distilled from NaK alloy under static vacuum and stored under Ar prior to use.

S1.2. Radiation protection. ^{99}Tc is a long-lived weak β^--emitter (E_{max} = 0.292 MeV). Normal glassware provides adequate protection against the beta radiation when milligram amounts are used. Secondary X-rays (Bremsstrahlung) play a significant role only when larger amounts of ^{99}Tc are handled. All manipulations were performed in a laboratory approved for the handling of radioactive materials.

S1.3. Synthetic procedures.

[Na(Crypt-2.2.2.)][Tc(CO)(CN*p*-F-Ar^{DArF2})$_4$] (2): TcCl(CO)(CN*p*-F-Ar^{DArF2})$_4$ (80 mg, 0.0343 mmol) and cryptand-2.2.2. (15 mg, 0.04 mmol) were dissolved in 3 ml THF and 200 µl Na/Hg (0.7%) were added. Vigorous stirring for 6 min. gave a black solution, which was decanted from the mercury phase. The volume was reduced to 0.5 ml *in vacuo*, toluene (0.5 ml) was added and the solution was cannula-filtered. Addition of pentane and storing at -20°C gave black single crystals of **2**. Yield: 56 mg (60%). ^{1}H NMR (THF-*d*$_8$, ppm): δ 7.76 and 7.73 (two overlapped s, 24H, Ph), 7.43 (d, *J* = 8 Hz, 8H, *Ar*-F). ^{19}F-NMR (THF-*d*$_8$, ppm): δ −63.2 (s, 48F, Ph–*CF*$_3$), −110.3 (t, *J* = 8 Hz, 4F, Ar–*F*). ^{99}Tc NMR (THF-*d*$_8$, ppm): δ −1876 (s), $\nu_{1/2}$ = 4394 Hz.

***trans*-[TcH(CO)(CN*p*-F-Ar^{DArF2})$_4$] (3):** To 3 ml of a frozen THF solution of [Na(Crypt-2.2.2.)][Tc(CO)(CN*p*-F-Ar^{DArF2})$_4$] (*in situ* prepared as described above), 350 µl HCl (Et_2O solution, 0.1 M) were added. The solution turned yellow upon thawing and was kept at room temperature overnight to complete the isomerization to the *trans* isomer. THF was evaporated *in vacuo* and benzene (2 ml) was added. The mixture was cannula-filtered and kept at room temperature overnight. The resulting yellow single crystals of **3** were filtered off and washed with pentane. Yield: 20 mg (26%). ^{1}H NMR (THF-*d*$_8$, ppm): δ 7.78 (s, 16H, Ph), 7.75 (s, 8H, Ph), 7.43 (d, *J* = 8 Hz, 8H, *Ar*–F), −5.26 (s, 1H, Tc–*H*). ^{19}F-NMR (THF-*d*$_8$, ppm): δ −63.3 (s, 48F, Ph–*CF*$_3$), −112.0 (t, *J* = 8 Hz, 4F, Ar–*F*).

[Tc(SnMe$_3$)(CO)(CN*p*-F-Ar^{DArF2})$_4$] (4): To 3 ml of a frozen THF solution of [Na(Crypt-2.2.2.)]-[Tc(CO)(CN*p*-F-Ar^{DArF2})$_4$] (*in situ* prepared as described above) 350 µl $ClSnMe_3$ (THF solution, 0.1 M) was added. The solution turned yellow-brown upon stirring at room temperature for 1.5 h. The solution was concentrated *in vacuo*, diluted with toluene and cannula-filtered. Storing at -20° C yielded yellow single crystals of **4**, which were filtered off and washed with pentane. Yield: 40 mg (16%). ^{1}H NMR (THF-*d*$_8$, ppm): δ 8.01 (broad, 16H, Ph), 7.76 (broad, 8H, Ph), 7.33 (broad, 8H, *Ar*–F), −1.79 (s, 3H, Sn–C*H*$_3$). ^{19}F-NMR (THF-*d*$_8$, ppm): δ −63.2 (broad, 48F, Ph–*CF*$_3$), −111.7 (t, *J* = 8 Hz, 4F, Ar–*F*). ^{99}Tc NMR (THF-*d*$_8$, ppm): δ −2171 (s), $\nu_{1/2}$ = 1214 Hz.

S2. Crystallographic Structure Determinations

S2.1. General. The intensities for the X–ray determinations were collected on a Bruker D8 Venture or on a Bruker APEX II Ultra instrument with Mo K_α or Cu K_α radiation. Structure solutions and refinements were performed with the SHELX program packages.[4,5] Hydrogen atoms were placed at calculated positions and treated with the 'riding model' option of SHELXL. The representations of molecular structures were done using the program DIAMOND (vers. 4.5.1).[6] Additional information on the structure determinations is has been deposited with the Cambridge Crystallographic Data Centre under the deposition numbers CCDC 2238710 (**2**), CCDC-2238711 (**3**) and CCDC-2238712 (**4**).

Table S2.1 Crystal data and structure determination parameters

	[Na(Cryp-2.2.2.)][Tc(CN*p*-F-Ar^{DArF2})$_4$(CO)] (**2**) x 0.25 toluene x 0.5 THF	*trans*-[TcH(CN*p*-F-Ar^{DArF2})$_4$(CO)] (**3**)	[Tc($SnMe_3$)(CN*p*-F-Ar^{DArF2})$_4$(CO)] (**4**) x toluene x 0.5 THF
Formula	$C_{114.75}H_{74}F_{52}N_6NaO_{7.5}Tc$	$C_{93}H_{32}F_{52}N_4OTc$	$C_{105}H_{53}F_{52}N_4O_{1.5}SnTc$
M_w	2765.79	2307.22	2599.20
Crystal system	monoclinic	triclinic	triclinic
a/Å	21.0710(4)	14.324(10)	14.727(5)
b/Å	23.6777(4)	15.260(9)	15.583(9)
c/Å	24.0500(5)	21.510(14)	50.04(3)
α	90	84.718(19)	94.762(7)
β	98.0673(12)	86.25(2)	96.185(10)
γ	90	73.327(19)	94.402(12)
V/ $Å^3$	11880.1(4)	4481(5)	11336(10)
Radiation	Cu K_α	Mo K_α	Mo K_α
Space group	$P2_1/n$	$P\bar{1}$	$P\bar{1}$
Z	4	2	4
ρ_{calc} g/cm^{-3}	1.546	1.710	1.523
No. reflect.	154012	178241	355824
No. indep.	22513	19699	49591
R_{int}	0.0918	0.1044	0.1169
No. param.	1574	1362	2806
R_1/wR_2 [I>2σ(I)]	0.0883/0.2425	0.0807/0.1893	0.1000/0.2248
GOF	1.022	1.085	1.050

S2.2 Disorder and Refinement Specifics. All structures contain rotational disorder of the trifluoromethyl groups, which were modeled and refined anisotropically. The solid-state structures of **2** suffered from translational disorder of the entire [Na(crypt-2.2.2.)]$^{+}$ cation, which was modeled with occupation probabilities of 0.67/0.33 for the two positions. 0.25 molecule of toluene and two 0.25 molecules of THF are co-crystallized with the salt. The electron density of the hydrido ligand in **3** could not be identified and the complex crystallized with pyramidal inversion disorder. The major {Tc(CO)} component was fully refined to 0.88 occupancy and only one component of the disorder model is shown. The solid-state structure of **4** contains two molecules in the asymmetric unit. One molecule is well ordered, while the second (not shown in the model) suffered from severe positional disorder at one flanking ring of one ligand; this was adequately modeled with a SAME instruction taking as reference the other identical molecule. Moreover, one molecules of toluene and ½ molecule of THF are co-crystallized per complex molecule.

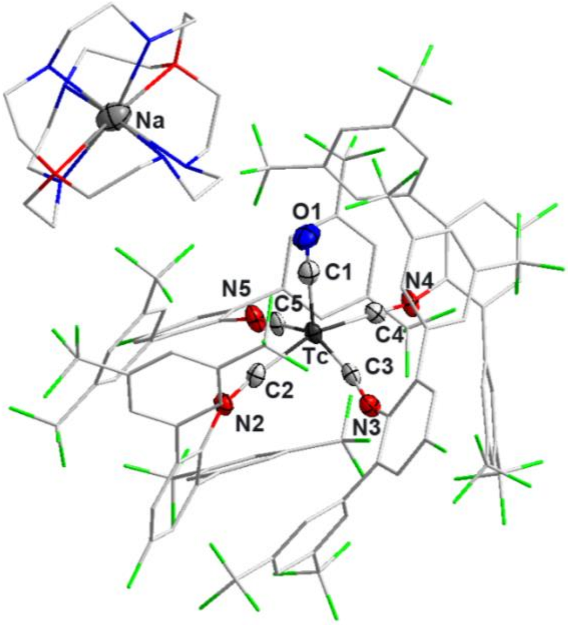

Figure S2.1. Molecular structure of [Na(Cryp-2.2.2.)][Tc(CO)(CN*p*-F-Ar$^{\mathrm{DArF2}}$)$_4$] (**2**). Hydrogen atoms are omitted for clarity.

Table S2.2. Selected bond lengths (Å) and angles (°) in [Na(Cryp-2.2.2.)][Tc(CO)(CN*p*-F-Ar$^{\mathrm{DArF2}}$)$_4$] (**2**).

Tc-C1	1.915(6)	Tc-C5	2.001(5)	C3-N3	1.205(7)
Tc-C2	1.978(5)	C1-O1	1.163(7)	C4-N4	1.182(7)
Tc-C3	1.958(6)	C2-N2	1.199(7)	C5-N5	1.182(7)
Tc-C4	1.984(5)				
Tc-C1-O1	177.5(5)	Tc-C4-N4	173.6(4)	C1-Tc-C3	99.2(2)
Tc-C2-N2	175.0(5)	Tc-C5-N5	179.3(5)	C1-Tc-C4	95.8(2)
Tc-C3-N3	171.2(4)	C1-Tc-C2	106.0(2)	C1-Tc-C5	109.6(2)

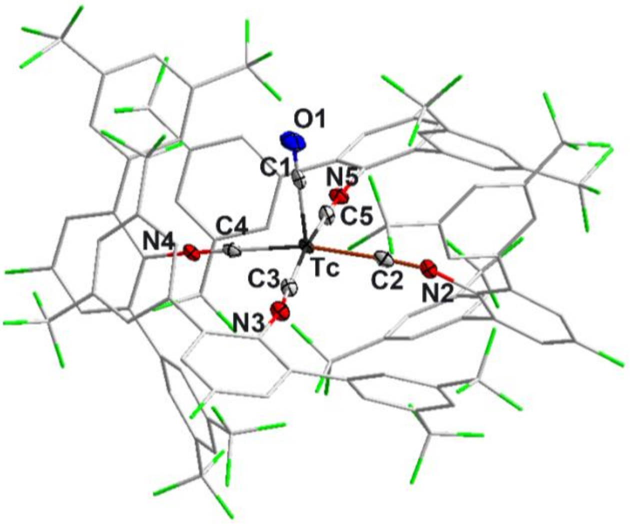

Figure S2.2. Molecular structure of *trans*-[TcH(CO)(CN*p*-F-Ar^{DArF2})$_4$] (**3**). Hydrogen atoms are omitted for clarity.

Table S2.3. Selected bond lengths (Å) and angles (°) in *trans*-[TcH(CO)(CN*p*-F-Ar^{DArF2})$_4$] (**3**).

Tc-C1	1.975(6)	Tc-C5	2.026(5)	C3-N3	1.171(6)
Tc-C2	2.019(5)	C1-O1	1.144(7)	C4-N4	1.172(6)
Tc-C3	2.026(5)	C2-N2	1.156(6)	C5-N5	1.164(6)
Tc-C4	2.010(5)	TcA-C1A	1.966(15)	TcA-C2	2.001(7)
TcA-C3	2.040(7)	TcA-C5	2.046(7)	C1A-O1A	1.161(18)
TcA-C4	1.998(7)				
Tc-C1-O1	176.2(5)	Tc-C4-N4	175.1(4)	C1-Tc-C3	97.3(2)
Tc-C2-N2	173.3(4)	Tc-C5-N5	178.8(4)	C1-Tc-C4	99.6(2)
Tc-C3-N3	178.7(4)	C1-Tc-C2	97.1(2)	C1-Tc-C5	90.8(2)
TcA-C1-O1		TcA-C4-N4	162.7(4)	C1A-TcA-C3	106.5(9)
TcA-C2-N2	163.3(4)	TcA-C5-N5	167.7(4)	C1A-TcA-C4	96.1(9)
TcA-C3-N3	168.4(5)	C1A-TcA-C2	93.3(9)	C1A-TcA-C5	90.2(9)

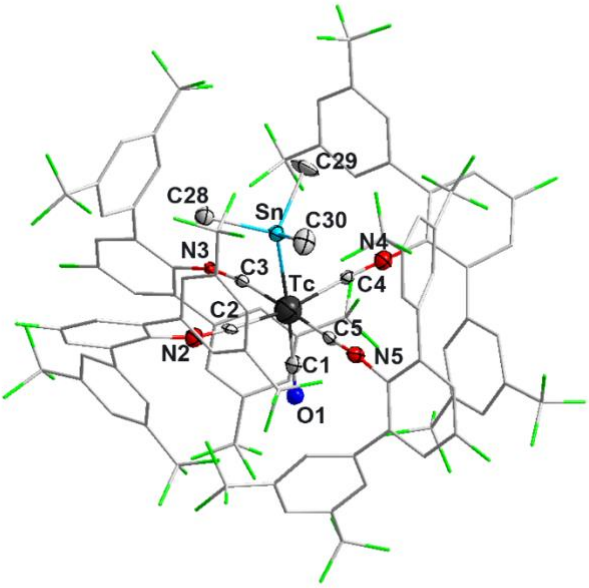

Figure S2.3. Molecular structure of *trans*-[Tc(SnMe$_3$)(CO)(CN*p*-F-Ar$^{\mathrm{DArF2}}$)$_4$] (**4**). Hydrogen atoms are omitted for clarity.

Table S2.4. Selected bond lengths (Å) and angles (°) in *trans*-[Tc(SnMe$_3$)(CO)(CN*p*-F-Ar$^{\mathrm{DArF2}}$)$_4$] (**4**).

Tc-C1	1.954(7)	Tc-C5	2.036(6)	C3-N3	1.171(8)
Tc-C2	2.013(6)	C1-O1	1.141(8)	C4-N4	1.177(8)
Tc-C3	2.015(6)	C2-N2	1.184(8)	C5-N5	1.168(8)
Tc-C4	2.033(6)	TcA-C1A	1.935(10)	TcA-C2A	2.024(7)
TcA-C3A	2.026(8)	TcA-C5A	2.015(9)	C1A-OA	1.175(11)
TcA-C4A	2.025(8)	Sn-Tc	2.7491(10)	SnA-TcA	2.7473(13)
Tc-C1-O1	176.8(7)	Tc-C4-N4	173.7(5)	C1-Tc-C3	92.2(3)
Tc-C2-N2	175.5(5)	Tc-C5-N5	170.6(5)	C1-Tc-C4	96.5(3)
Tc-C3-N3	177.0(6)	C1-Tc-C2	97.7(3)	C1-Tc-C5	89.9(3)
TcA-C1A-OA	179.0(9)	TcA-C4A-N4A	175.1(9)	C1A-TcA-C3A	87.2(3)
TcA-C2A-N2A	176.5(6)	TcA-C5A-N5A	175.5(7)	C1A-TcA-C4A	99.0(4)
TcA-C3A-N3A	174.5(7)	C1A-TcA-C2A	96.1(3)	C1A-TcA-C5A	90.9(3)

S3. Nuclear magnetic resonance

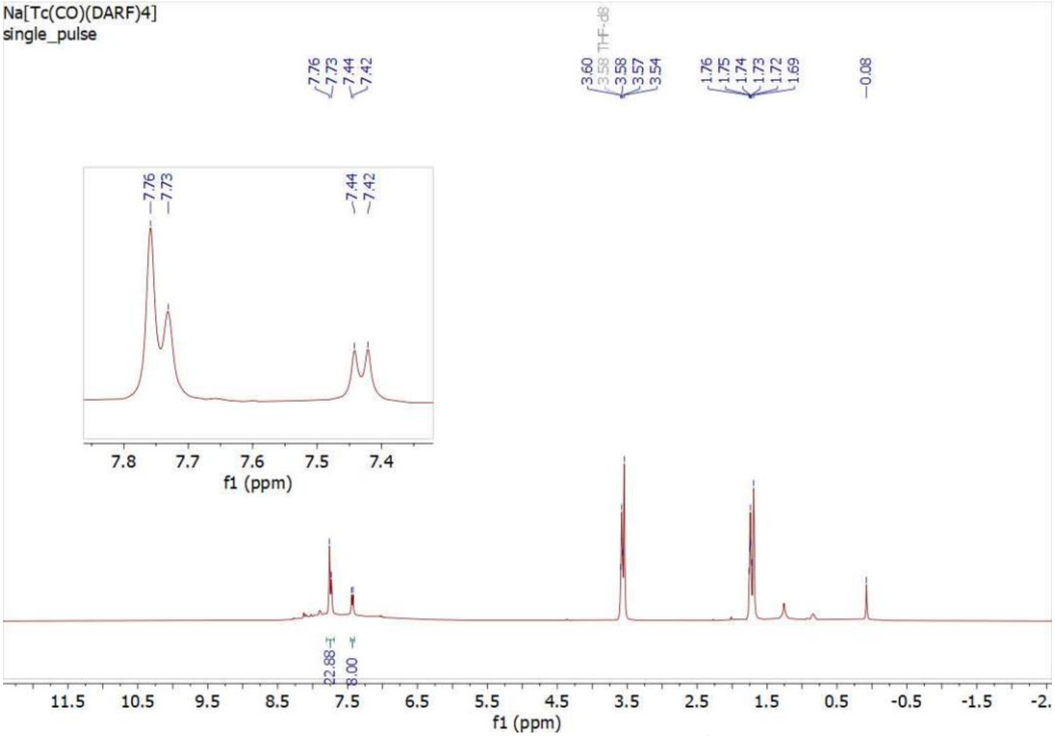

Figure S3.1. ^{1}H NMR spectrum of Na[Tc(CO)(CN*p*-F-Ar^{DArF2})$_4$] in THF-d$_8$

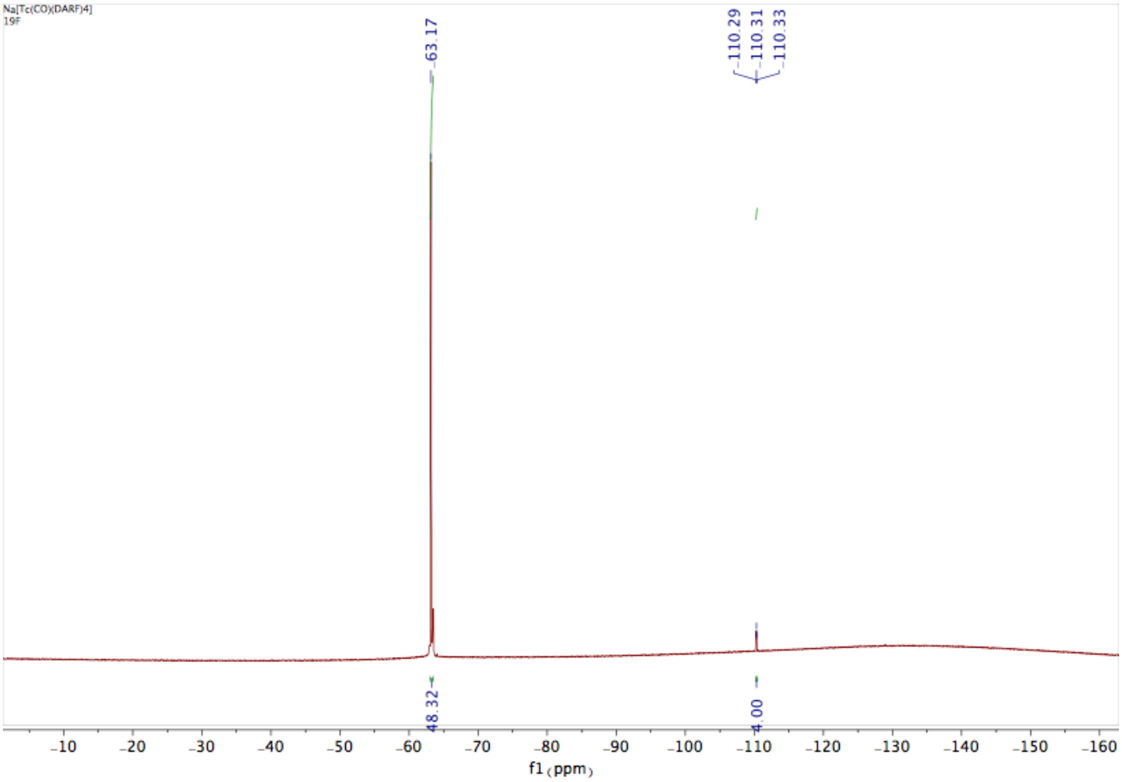

Figure S3.2. ^{19}F NMR spectrum of Na[Tc(CO)(CN*p*-F-Ar^{DArF2})$_4$] in THF-d$_8$

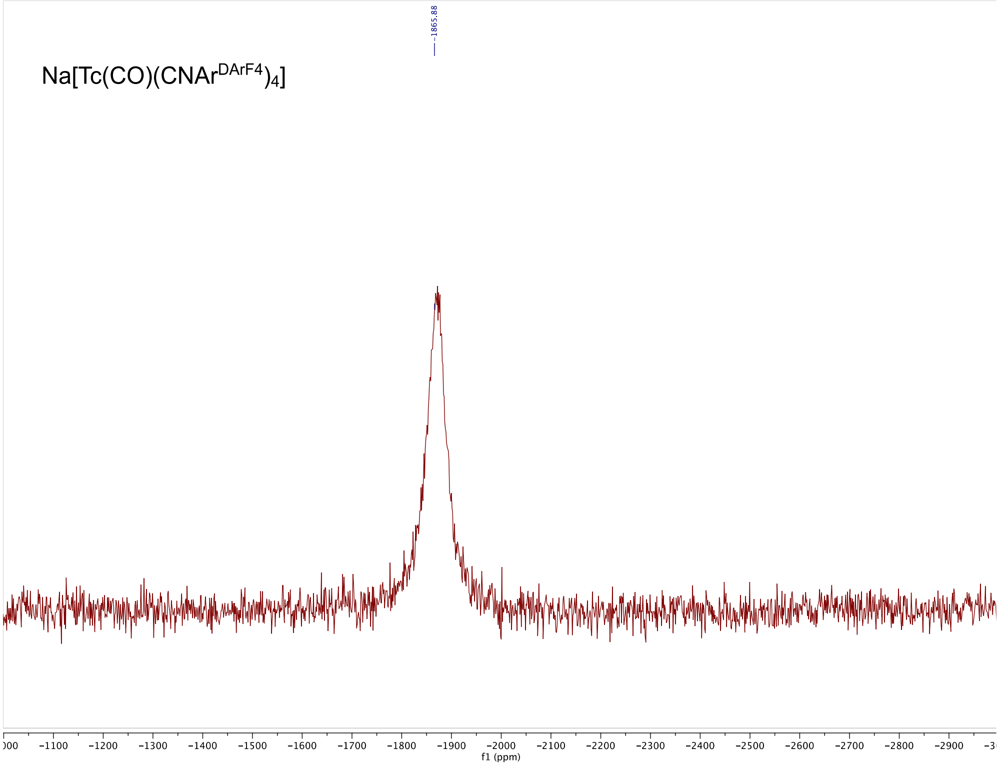

Figure S3.3. ^{99}Tc NMR spectrum of Na[Tc(CO)(CN*p*-F-Ar^{DArF2})$_4$] in THF-d_8

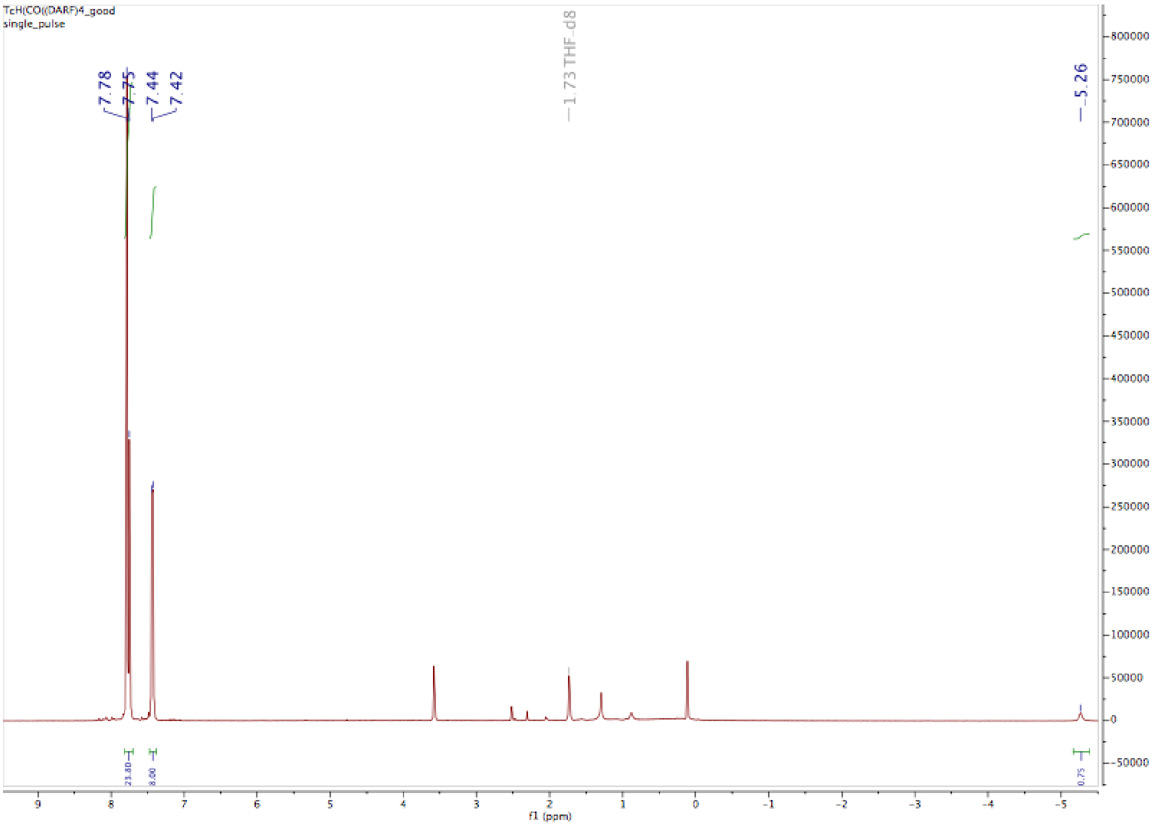

Figure S3.4. ^{1}H NMR spectrum of *trans*-[TcH(CO)(CN*p*-F-Ar^{DArF2})$_4$] in THF-d_8

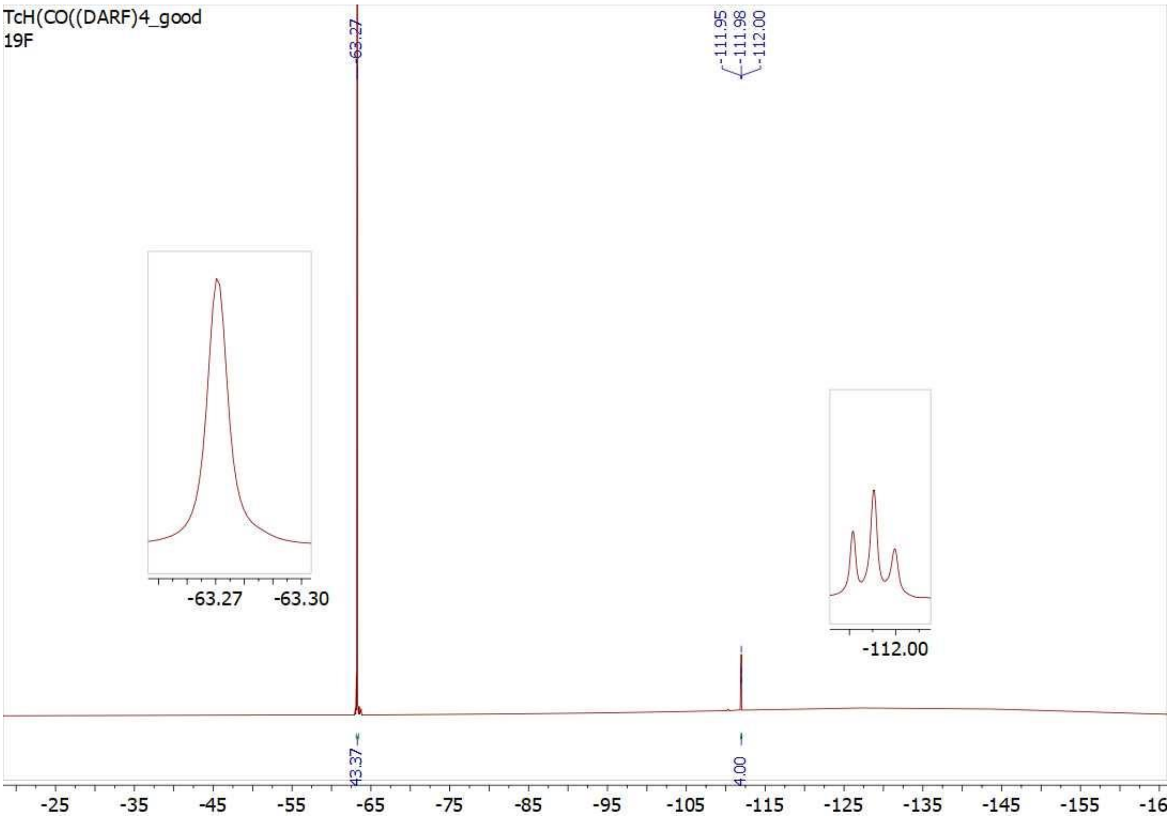

Figure S3.5. ^{19}F NMR spectrum of *trans*-[TcH(CO)(CN*p*-F-Ar^{DArF2})$_4$] in THF-d$_8$

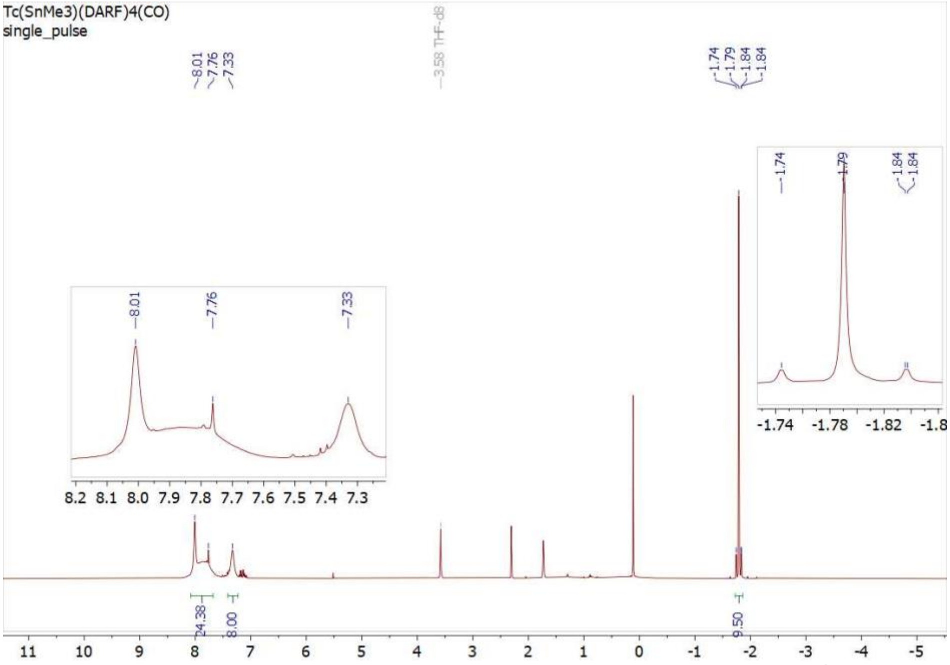

Figure S3.6. ^{1}H NMR spectrum of *trans*-[Tc(SnMe$_3$)(CO)(CN*p*-F-Ar^{DArF2})$_4$] in THF-d$_8$

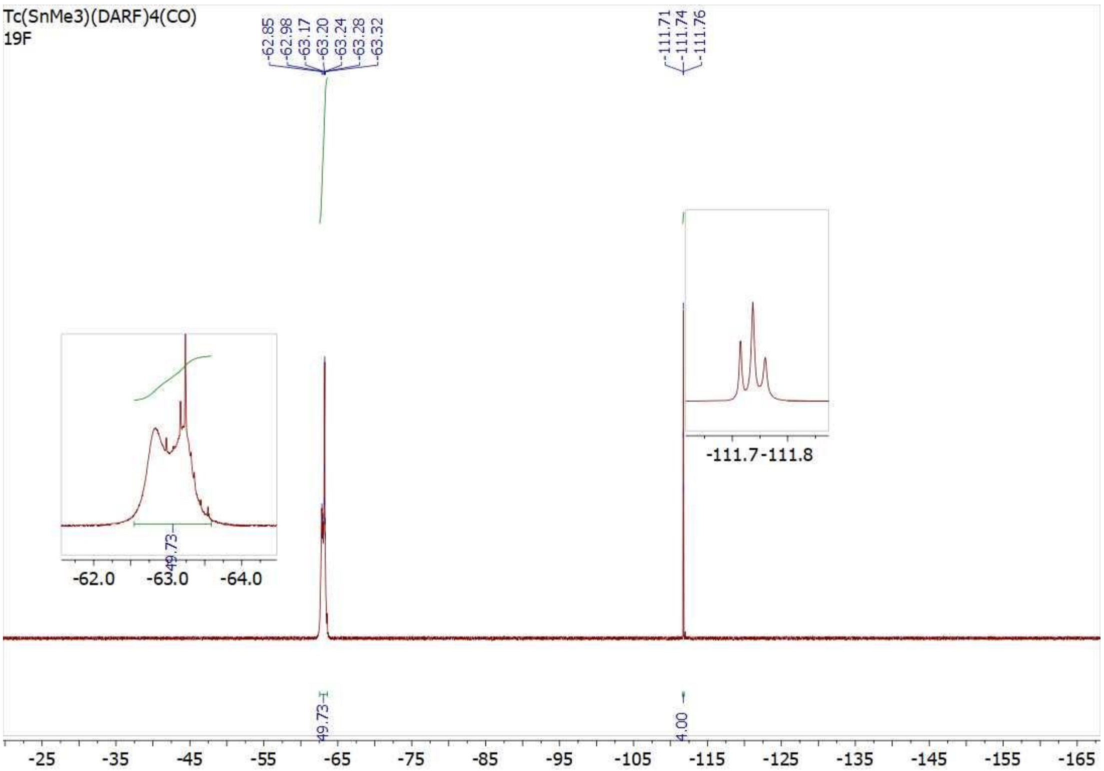

Figure S3.7. ^{19}F NMR spectrum of *trans*-[Tc(SnMe$_3$)(CO)(CN*p*-F-Ar^{DArF2})$_4$] in THF-d$_8$

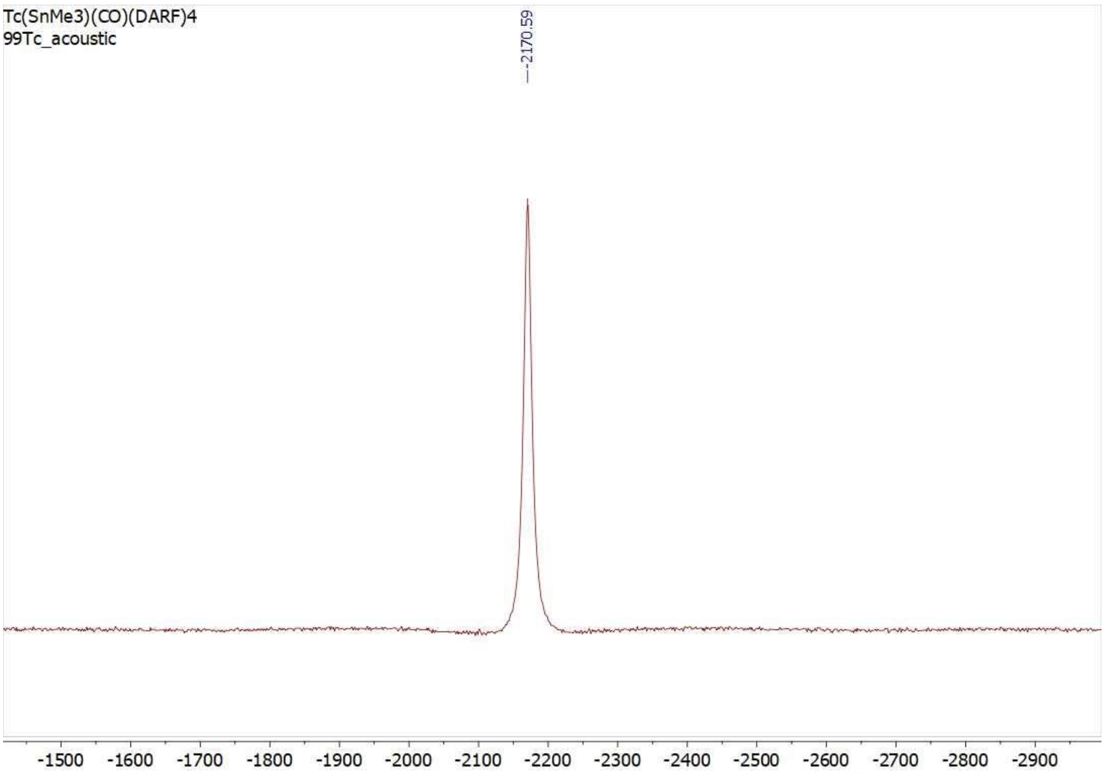

Figure S3.7. ^{99}Tc NMR spectrum of *trans*-[Tc(SnMe$_3$)(CO)(CN*p*-F-Ar^{DArF2})$_4$] in THF-d$_8$

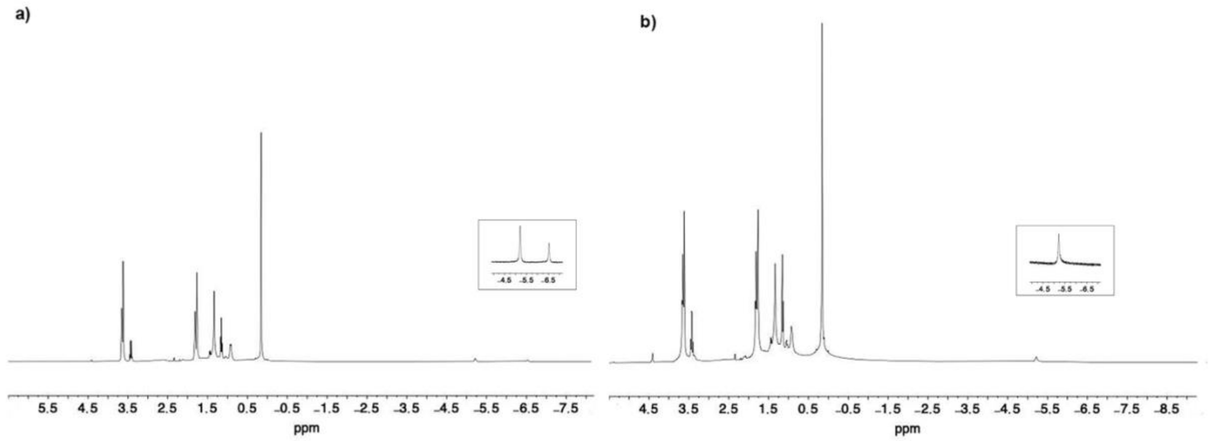

Figure S3.8. ^{1}H NMR spectra of a reaction mixture of and ethereal HCl in THF-d_8 a) after 1 h and b) after 24h illustrating the intermediate formation of a *cis* isomer, which isomerized within 24 h to the isolated *trans*-[TcH(CO)(CN*p*-F-Ar^{DArF2})$_4$].

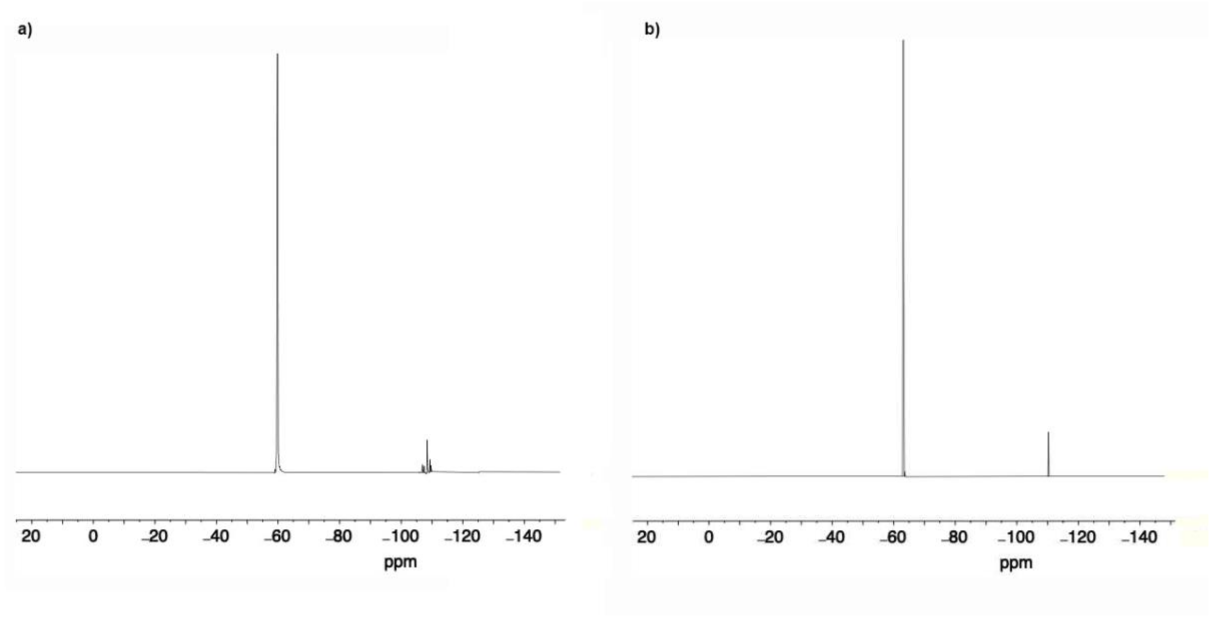

Figure S3.9. ^{19}F NMR spectra of a reaction mixture of and ethereal HCl in THF-d_8 a) after 1 h and b) after 24h illustrating the intermediate formation of a *cis* isomer, which isomerized within 24 h to the isolated *trans*-[TcH(CO)(CN*p*-F-Ar^{DArF2})$_4$]. Note the sensitivity of the phenyl-bonded fluorine atom (about 110 ppm) for structural changes .

S4. References

[1] T. B. Ditri, A. E. Carpenter, D. S. Ripatti, C. E. Moore, A. L. Rheingold, J. S. Figueroa, *Inorg. Chem.*, 2013, **52**, 13216-13229.

[2] S. Hildebrandt, PhD Thesis, FU Berlin, 2018,

[3] F. Salsi, M. Neville, M. Drance, A. Hagenbach, J. S. Figueroa, U. Abram, *Organometallics,* 2021, **40**, 1336-1343.

[4] G. M. Sheldrick, *Acta Crystallogr., Sect. A,* 2008, **64**, 112-122.

[5] G. M. Sheldrick, *Acta Crystallogr., Sect. C: Struct. Chem.* 2015, **71**, 3-8.

[6] K. Brandenburg, *Diamond- Crystal and Molecular Structure Visualization*, version 4.5.1; Crystal impact GbR: Bonn, Germany, 2018.